Geo-Mar Lett (2013) 33:233–243
DOI 10.1007/s00367-013-0321-7

ORIGINAL

Fungal colonies in open fractures of subseafloor basalt

Magnus Ivarsson · Stefan Bengtson · Henrik Skogby · Veneta Belivanova · Federica Marone

Received: 13 September 2012 / Accepted: 25 January 2013 / Published online: 3 February 2013

Abstract The deep subseafloor crust is one of the few great frontiers of unknown biology on Earth and, still today, the notion of the deep biosphere is commonly based on the fossil record. Interpretation of palaeobiological information is thus central in the exploration of this hidden biosphere and, for each new discovery, criteria used to establish biogenicity are challenged and need careful consideration. In this paper networks of fossilized filamentous structures are for the first time described in open fractures of subseafloor basalts collected at the Emperor Seamounts, Pacific Ocean. These structures have been investigated with optical microscopy, environmental scanning electron microscope, energy dispersive spectrometer, X-ray powder diffraction as well as synchrotron-radiation X-ray tomographic microscopy, and interpreted as fossilized fungal mycelia. Morphological features such as hyphae, yeast-like growth and sclerotia were observed. The fossilized fungi are mineralized by montmorillonite, a process that probably began while the fungi were alive. It seems plausible that the fungi produced mucilaginous polysaccharides and/or extracellular polymeric substances that attracted minerals or clay particles, resulting in complete fossilization by montmorillonite. The findings are in agreement with previous observations of fossilized fungi in subseafloor basalts and establish fungi as regular inhabitants of such settings. They further show that fossilized microorganisms are not restricted to pore spaces filled by secondary mineralizations but can be found in open pore spaces as well. This challenges standard protocols for establishing biogenicity and calls for extra care in data interpretation.

M. Ivarsson (✉) · S. Bengtson
Department of Palaeozoology and Nordic Center for Earth Evolution (NordCEE), Swedish Museum of Natural History, P.O. Box 50007, 10405 Stockholm, Sweden
e-mail: magnus.ivarsson@nrm.se

H. Skogby
Department of Mineralogy, Swedish Museum of Natural History, Stockholm, Sweden

V. Belivanova
Department of Palaeozoology, Swedish Museum of Natural History, Stockholm, Sweden

F. Marone
Swiss Light Source, Paul Scherrer Institute, Villigen, Switzerland

Introduction

Traces of microbial activity in subseafloor basalts are commonly preserved either as granular or tubular ichnofossils in volcanic glass (e.g. Furnes et al. 2008; Staudigel et al. 2008; McLoughlin et al. 2009) or as body fossils in veins and vesicles filled by secondary carbonates (Schumann et al. 2004; Ivarsson and Holm 2008; Ivarsson et al. 2008a, 2008b; Peckmann et al. 2008; Eickmann et al. 2009; Cavalazzi et al. 2011). Ivarsson et al. (2008a, 2008b) described filamentous fossilized microorganisms from the Emperor Seamounts in the Pacific Ocean in carbonate-filled veins and vesicles to a depth of ~900 metres below seafloor (mbsf). These fossilized microorganisms were associated with high amounts of carbon, phosphates and hydrocarbons, as well as possible lipids and DNA. The microorganisms were interpreted to have lived in the veins and vesicles within circulating hydrothermal fluids. At some point, carbonate saturation was reached and the carbonates were precipitated. Fluid-inclusion studies showed the carbonate formation to have been a quick event, and the microorganisms were instantly entombed and preserved, resulting in high content of organic remains (Ivarsson et al. 2009). The fossils were later reinterpreted as fungal hyphae, rather than filamentous prokaryotes (Ivarsson et al. 2012), based on characteristic fungal morphologies including septa and anastomoses, and the detection of chitin in the cell walls with the dye WGA-FITC. Ivarsson (2012) further described fossilized fruiting bodies and spores associated with the hyphae, which indicates that these fungi existed in vital colonies in subseafloor basalts between ~81 and 48 Ma (cf. (Tarduno et al. 2002).

The fossilized microorganisms were preserved as Si, Al, Fe clay-like phases, iron oxides and remnants of organic compounds. In the Rheinisches Schiefergebirge of Germany, Peckmann et al. (2008) described fossilized filamentous microorganisms with a similar composition from an ophiolite. Based on energy dispersive spectrometer (EDS) data, they calculated them to consist of the clay minerals illite and chamosite. They further suggested that the clay composition was the result of microbial clay authigenesis.

Despite notable progress during the last decade, substantial gaps in the understanding of the deep biosphere of subseafloor basalts still exist. The abundance, diversity and biogeochemical consequences of subseafloor life are not well known. Moreover, methods to sample and study the deep biosphere without contamination are not yet fully developed. Thus, current knowledge of the subseafloor biosphere is based mainly on fossilized material. In the present paper complex networks of fossilized filamentous structures are examined in samples from the Emperor Seamounts in which Ivarsson et al. (2012) had already observed fossilized fungal mycelia preserved in vesicle-filling minerals. If such structures were to occur also in open vesicles, it would challenge standard protocols for establishing biogenicity and call for extra care in data interpretation.

Study area

Together with the Hawaiian Islands, the Emperor Seamounts form a continuous chain of volcanic seamounts and islands that extends over 5,000 km in the Pacific Ocean. The chain is considered to be the result of hotspot volcanism, and the ages increase successively in a classical fashion to the northwest away from the active hotspot at Loihi Seamount.

During Ocean Drilling Program (ODP) Leg 197, the Detroit, Nintoku and Koko seamounts were drilled. Sites 1203 and 1204 are at the summit of Detroit Seamount. Site 1203 was drilled to a final depth of 914.6 mbsf. Site 1204 consists of two drill holes, 1204A and 1204B, with total depths of 880.3 and 954.5 mbsf respectively. Site 1205 was drilled on Nintoku Seamount to a final depth of 326.0 mbsf, and site 1206 on Koko Seamount to a final depth of 335.2 mbsf.

Detroit Seamount has been radiometrically dated during ODP Leg 145 (site 884) to an age of ~81 Ma. Nintoku Seamount has been dated to 56 Ma and Koko Seamount to 48 Ma during ODP Leg 197. The samples thus stretch over a time period of 33 Ma (Tarduno et al. 2002).

Materials and methods

Seventy-two samples from all three seamounts were examined during this study. Seventeen of these contain open fractures with filamentous structures, and these samples were selected for further analysis (Table 1). All samples had been stored in sealed plastic bags and, thus, had not been exposed to the atmosphere prior to analysis, except for two samples: these had been used for preparation of thin sections in previous studies but, immediately after sawing, had been sealed again.

The samples were initially investigated under an optical light microscope and an environmental scanning electron microscope (ESEM). Some were cut into smaller pieces to fit in the ESEM or for the purpose of investigating the interior of the samples. Some large fractures were also split open mechanically. Mineral phases were identified and studied by a combination of microscope, EDS and X-ray powder diffraction (XRD) analyses. The fossilized filamentous structures were characterized by using optical microscopy, ESEM/EDS and synchrotron-based X-ray tomographic microscopy (SRXTM).

An XL30 ESEM with a field emission gun was used to analyse the minerals and the filamentous structures. The ESEM was equipped with an Oxford x-act EDS, a backscatter electron detector and a secondary electron detector. The acceleration voltage was 20 or 15 kV depending on the nature of the sample, and the instrument was calibrated with a cobalt standard. Peak and element analyses were made using INCA Suite 4.11 software.

Table 1 Overview of the samples used in this study, including depth and description of pore spaces

Samples (197-)	Depth (mbsf)	Veins and/or vugs
1203		
1203A-52R-2, 57	762.3	Veins and vugs
1203A-52R-3, 40	763.7	Veins and vugs
1203A-53R-2, 43	771.9	Veins and vugs
1203A-64R-2, 62	868.0	Veins and vugs
1204		
1204A-7R-2, 3	820.9	Veins and vugs
1204B-3R-3, 21	832.8	Vugs
1205		
1205A-5R-2, 60	33.9	Vugs
1205A-30R-1, 9	206.1	Vugs
1205A-32R-5, 25	222.9	Vugs
1205A-34R-5, 33	240.4	Veins and vugs
1205A-42R-2, 48	294.3	Vugs
1206		
1206A-4R-2, 0	67.5	Vugs
1206A-8R-3, 40	93.4	Vugs
1206A-17R-1, 33	142.8	Vugs
1206A-26R-1, 116	210.2	Vugs
1206A-35R-3, 110	279.8	Vugs
1206A-36R-1, 60	285.8	Vugs

X-ray powder diffraction data were acquired using CuK radiation and a Philips PW1050 goniometer equipped with a graphite monochromator. A background-free Si holder was used for samples that could be extracted only in small quantities.

For SRXTM analysis, the samples were reduced in size and mounted on a 3-mm-wide brass peg (Donoghue et al. 2006). Analyses were performed by means of the TOMCAT beamline at the Swiss Light Source, Paul Scherrer Institute (Stampanoni et al. 2006). The X-ray energy was optimized for maximum contrast at 13–20 kV. In all, 1,501 projections were acquired equiangularly over 180°, online post-processed, and rearranged into flat- and darkfield-corrected sinograms. Reconstruction was performed on a Linux PC farm using highly optimized routines based on the Fourier Transform method (Marone and Stampanoni 2012). Slice data derived from the scans were then assessed by means of Avizo® software (http://www.vsg3d.com/). With the 20× lens used, the resulting voxel size was 0.37 μm.

Results

Vesicles

The vesicles are from ~1 mm to several centimetres in diameter and connected by micrometre- to millimetre-sized fractures. The vesicle walls are covered by a thin (10–20 μm) crust of montmorillonite (Fig. 1). The remaining space of the vesicles is partially filled with calcite or zeolites. Scalenohedral calcite occurs as semi-transparent, millimetre-sized dog-tooth crystals on the vesicle walls. The zeolites also occur as millimetre-sized crystals of chabazite and natrolite on the vesicle walls (Fig. 1). Chabazite occurs as euhedral crystals, transparent or semi-transparent. Natrolite is fibrous and white opaque. Because of the working distance, the EDS analyses of the zeolites were imprecise but Si, Al, Na, Ca and K were detected, consistent with chabazite and natrolite composition.

Fossilized networks

The walls of the vesicles and some of the connecting veins are covered by networks of interconnected filamentous structures associated with globular clusters (Fig. 2). These networks are usually dense and compact, and firmly anchored in the clay phase of the vesicle walls or in the calcite and/or zeolite crystals. In some vesicles the networks are restricted to only one spot of the vesicle wall (Fig. 2a, b), whereas in others they cover the entire wall (Fig. 2c, d). The filamentous structures branch frequently, and anastomoses between branches are common, which results in a mycelium-like appearance of the networks (Fig. 2). The diameter of the filaments varies from 5–10 μm close to the vesicle walls to 10–20 μm further out from the walls. The length of the filaments varies as well but is usually between 100 and 500 μm. In cross section the filaments usually have an organized interior with a central strand about half of the total diameter of the filamentous structure (Fig. 3a). A few filaments have septum-like features (Fig. 3b).

At places filaments converge to form a web-like structure (Fig. 3c), commonly associated with spherical or irregular structures varying from 50 μm to 1 mm in diameter. There are two different types of spherical structures, with diffuse transitions between both. The first type consists of one or a few spherical structures with rather distinct round or oval shapes and smooth surfaces (Fig. 4). These bodies range in diameter between 100 and 500 μm and have a relatively

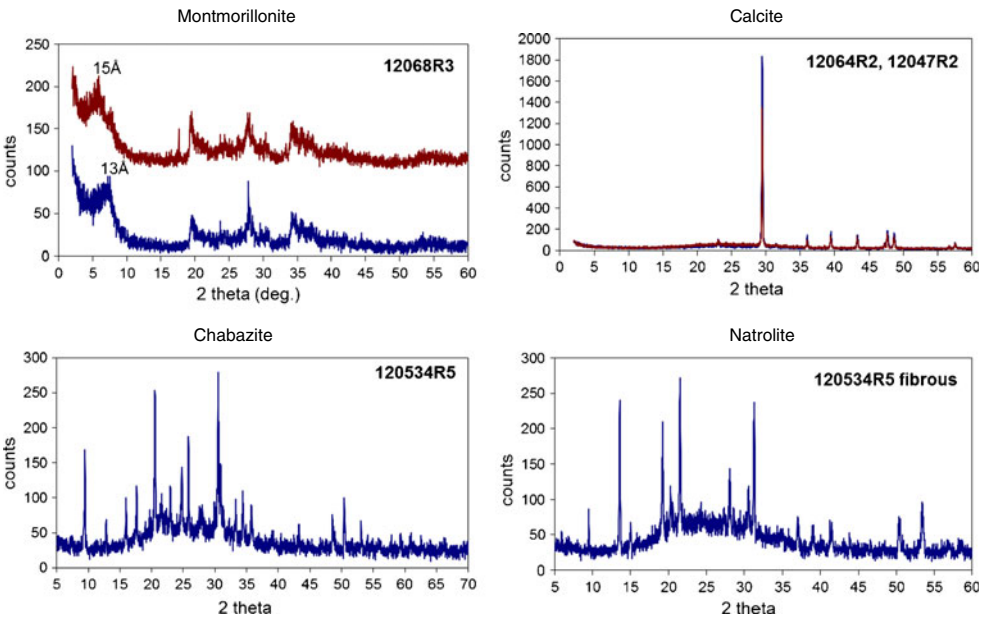

Fig. 1 Powder XRD diffractograms of montmorillonite, calcite, chabazite and natrolite. Montmorillonite: note change of basal reflection from 13 Å for dry sample (*bottom*) to 15 Å for moist sample (*top*), indicating basal swelling typical of montmorillonite. The diffractograms display relatively low signal/noise ratios due to the small amount of available sample material

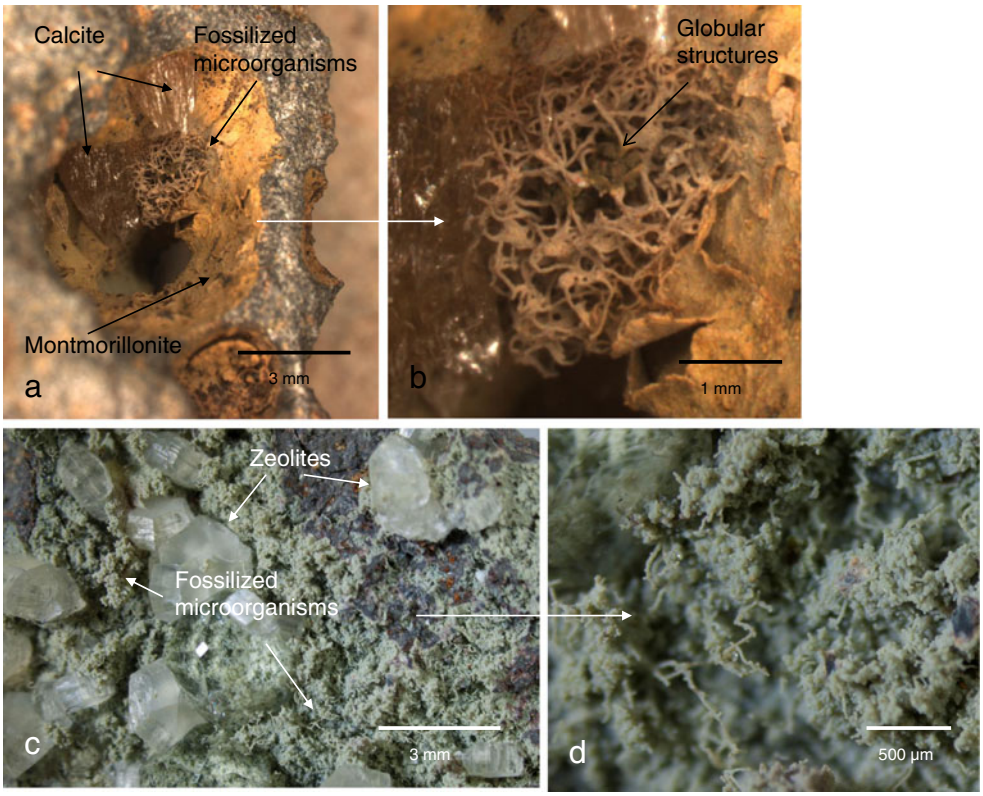

Fig. 2 Microphotographs of fossilized networks in open vesicles and veins in subseafloor basalt. **a**, **b** Sample 197-1206-4R-2: dense network of interconnected fossilized hyphae, tissue structures and spherical structures restricted to a single spot on the vesicle wall; the latter is lined with montmorillonite, and a few calcite crystals are present. **c**, **d** Sample 197-1205-34R-5: side of large fracture that has been cracked open; the fracture wall is covered with zeolite crystals, and a coherent network of fossilized filaments and cluster-like structures that extend throughout the fracture

thick rind and a massive interior (Fig. 4d). Some have more defined layers parallel to the rind and an inner part with diffuse morphologies. There are distinct colour variations between these layers. The rind is dark, almost black, the next layer light brown to yellowish and the inner core darker red-brown. Because of the working distance, EDS analyses

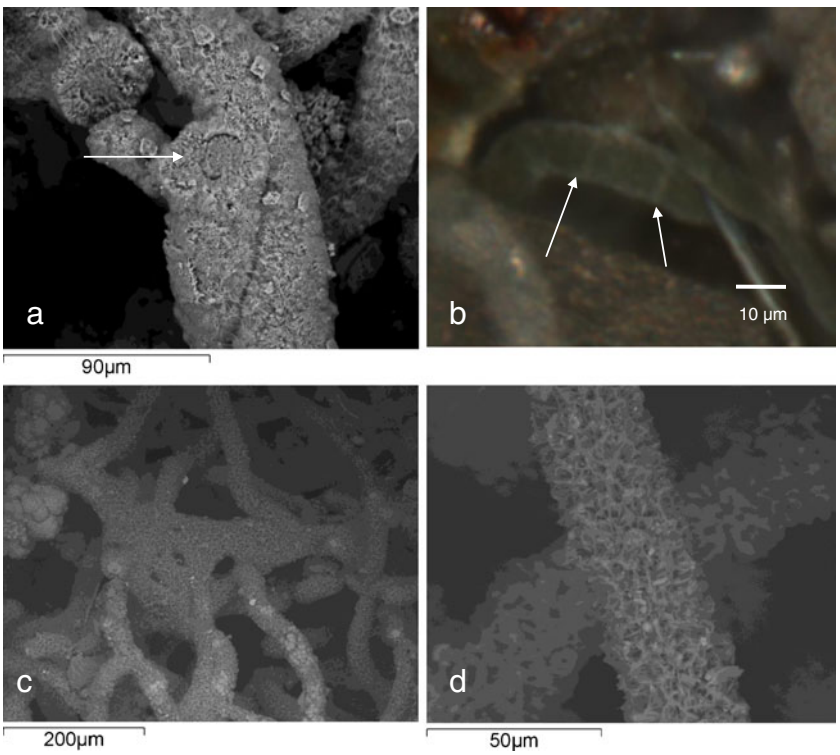

Fig. 3 ESEM images and microphotograph of fossilized filamentous structures: **a**, **b** sample 197-1205-34R-5; **c**, **d** sample 197-1206-4R-2. **a** ESEM image showing a cross section of a filament with a central strand. **b** Optical microphotograph of a filamentous structure showing septa. **c** ESEM image showing a web-like convergence of several filamentous structures. **d** ESEM close-up image of a fossilized filamentous structure showing mineralization of montmorillonite

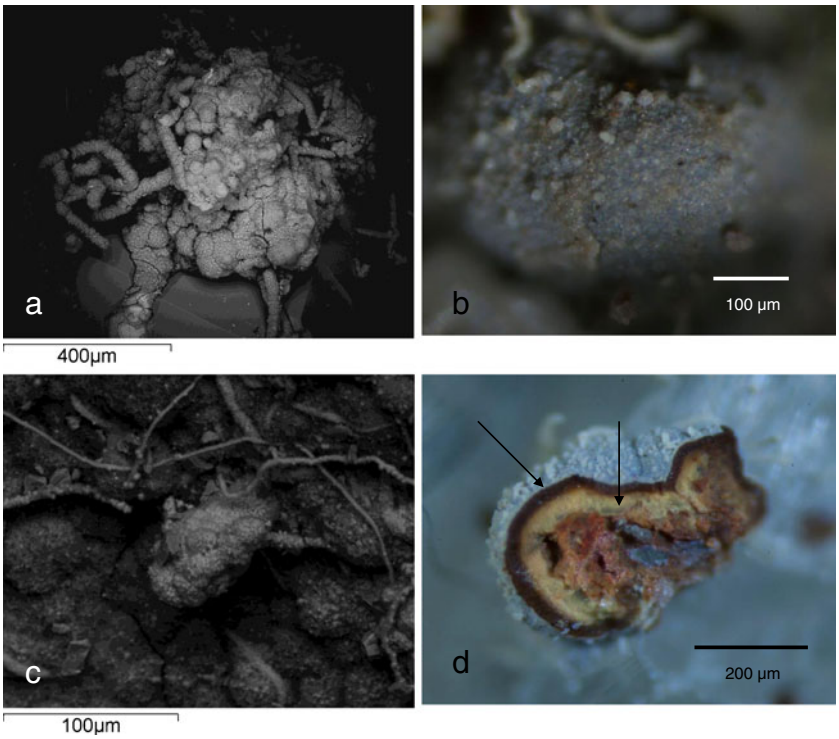

Fig. 4 ESEM images and microphotograph of spherical structures: **a**, **b**, **d** sample 197-1205-34R-5; **c** sample 197-1206-4R-2. **a** ESEM image showing a large, spherical, cluster-like structure attached to a zeolite surface; fossilized filamentous structures protrude from everywhere and into the underlying mineral. **b** Microphotograph of a spherical structure with a smooth surface. **c** ESEM image of a spherical structure attached to vein walls, with several filamentous structures protruding. **d** ESEM cross section of a spherical structure showing the internal layers, with a dark rind outermost, followed by a lighter layer and then a brown-reddish core probably of iron oxyhydroxides

were not possible on these various layers but the yellow-red-brown colours most likely reflect iron content. Colour changes can be due to variations in iron content or crystallinity, or between iron oxides and iron oxyhydroxides.

The second type consists of single spherical structures densely packed together into irregular clusters (Fig. 5). The single spheres range in diameter between 20 and 50 µm but the clusters can be as much as 1 mm in diameter. These clusters can build up on top of each other, forming almost tower-like mounds that reach several hundred micrometres in height (Fig. 5d–f). In other cases the clusters occur as dense assemblages in the middle of the filamentous networks.

Both types of spherical structures are closely associated to and connected with filaments. The smaller, single spheres form more or less indistinct transitions to the filaments or appear budded from the filaments, whereas the larger structures contain protruding filaments. Both types may be localized in the middle of the network but, more commonly, they are attached to a mineral surface. On top of several zeolite surfaces, large spherical structures occur with filaments protruding in all directions.

According to the XRD analyses, the filaments consist of a clay phase that corresponds to montmorillonite identical to that covering the vesicle walls. Because of the working distance, the ESEM/EDS analyses of the filamentous structures were imprecise. However, the analyses show consensus, and the filamentous structures appear to be composed of Si, Fe, Mg, Al and O as well as traces of K, Na and Ca. No C was detected.

SRXTM

Compared to the optical microphotographs and ESEM images, the SRXTM images considerably enhance the appearance of the morphology. The three-dimensional (3D) structure of the fossilized mycelium is more visible (Fig. 6a, b), including common features such as frequent branching and anastomoses between branches (Fig. 6c). It is easier to follow transitions between various morphological structures such as filaments and small spherical structures (Fig. 6a), or filaments and web-like structures (Fig. 6b). The distinct difference between small (Fig. 6a) and large spherical structures (Fig. 6d) is also clearly visualized by SRXTM.

To further exploit these three-dimensional data, stereo anaglyphs for the use of 3D glasses (red-cyan) have been added in Fig. 7.

Discussion

Biogenicity of putative fossilized microorganisms

The establishment of biogenicity of putative fossilized microorganisms is a complex and often controversial issue. Several sets of criteria have been formulated to discriminate between abiotic and biotic structures in sedimentary rocks (Schopf and Walter 1983; Buick 1991; Gibson et al. 2001). By contrast, Ivarsson (2006) focused on crystalline rocks: (1) is the geologic context compatible with life? (2) Is the

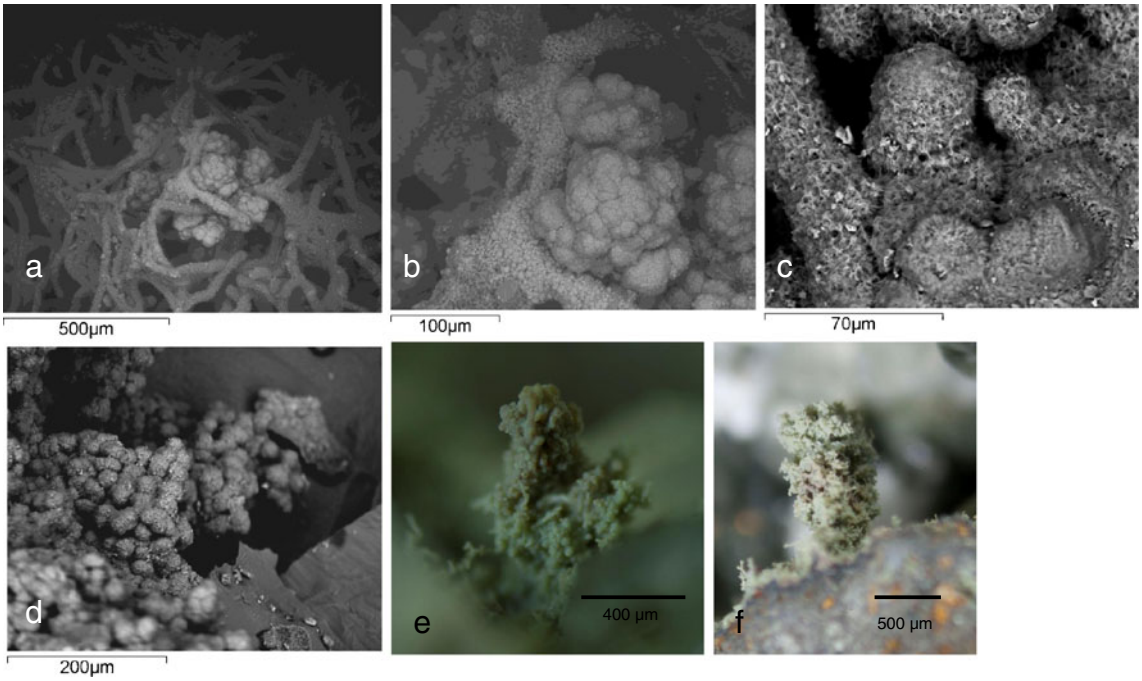

Fig. 5 ESEM images and microphotographs of clusters of densely packed spherical structures: **a**, **b** sample 197-1206-4R-2; **c**–**f** sample 197-1205-34R-5. **a** ESEM image of a cluster of spherical structures in the middle of a network of filamentous structures. **b** Close-up of **a**. **c** ESEM close-up of a single spherical structure. **d** Cluster of spherical structures. **e**, **f** Microphotographs of tower-like cluster structures oriented perpendicular to a vein wall; both filamentous and spherical structures have been replaced by montmorillonite

putative microfossil indigenous to the rock (rather than being a modern contaminant)? Is the indigenous microfossil syngenetic with secondary minerals? (3) Does the sample contain evidence of microbiological morphology? (4) Do the fossil-like microstructures contain chemical remnants indicative of past life? Are any organic biomarkers present? (5) Is there evidence of structural remains of colonies or communities? (6) Is there any evidence of biominerals? All criteria are seldom possible to fulfil in a single study and should be regarded as guidance—the more are fulfilled, the better is the case for biogenicity. The following is a test of the filamentous structures described in this study against the above criteria.

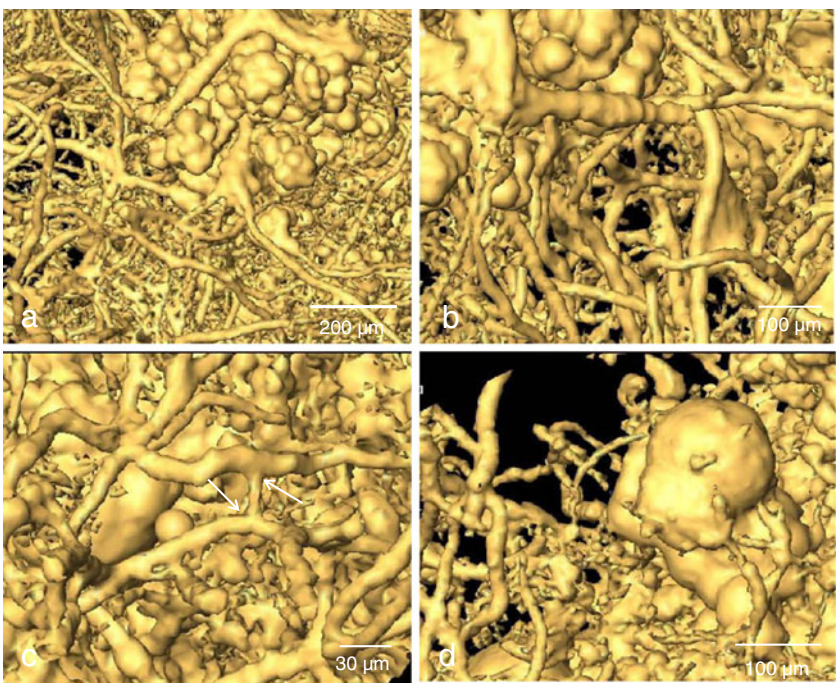

Fig. 6 Tomographic reconstructions (isosurface) of fossilized networks in sample 197-1206-4R-2. **a** Mycelium-like network of abundant hyphae and spherical structures densely packed together, forming irregular clusters; note the transitions between the hyphae and the spherical structures. **b** Filaments converging into a web-like substance in close association with spherical structures. **c** Anastomoses between branches. **d** Example of the larger type of spherical structures with rather distinct round or oval shapes and smooth surfaces

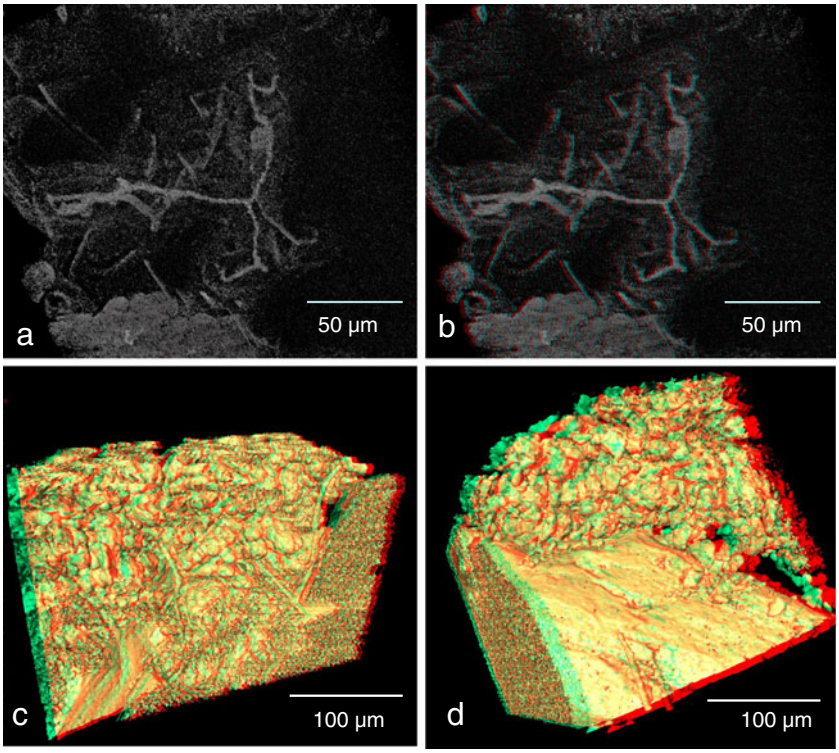

Fig. 7 Tomographic reconstructions (**a**, **b** voltex; **c**, **d** isosurface) of fossilized networks in sample 197-1206-4R-2. The three-dimensional effect can be viewed with the aid of 3D glasses. **a**, **b** Fossilized hyphae showing anastomoses: **a** without 3D effect, **b** with. **c** Fossilized hyphae associated with abundant spherical structures densely packed together, forming irregular clusters (yeast-like growth). **d** Hyphae and spherical structures in relation to a mineral surface

(1) During the last two decades, subseafloor settings have been shown to harbour a deep biosphere in the basaltic basement (e.g. Thorseth et al. 2001; Lysnes et al. 2004; Santelli et al. 2008). Observations of microbial activity in the oceanic basement usually concern granular or tubular ichnofossils in volcanic glass (e.g. Furnes et al. 2008; McLoughlin et al. 2009) but body fossils have also been reported (e.g. Al-Hanbali et al. 2001; Thorseth et al. 2001, 2003). Such fossilized microorganisms have been found in carbonate- and zeolite-filled veins and vugs in subseafloor basalts (e.g. Ivarsson and Holm 2008; Ivarsson et al. 2008a, 2008b; Cavalazzi et al. 2011) and in ophiolites (e.g. Peckmann et al. 2008; Eickmann et al. 2009), and have been associated with high amounts of carbon, phosphates, hydrocarbons and chitin as well as lipids and DNA (e.g. Ivarsson and Holm 2008; Ivarsson et al. 2008a, 2008b, 2012). Thus, subseafloor basement down to at least 900 m depth below seafloor is today recognized as a niche for microbial life, and the geological context of the present sample set is compatible with life.

(2) When studying fossilized microorganisms, the normal strategy is to observe them preserved and embedded in a mineral phase that can be directly dated or at least associated with a geological process or context that, in turn, can be correlated with a geological event or age. This is the case for fossilized microorganisms previously observed at sites 1203, 1204, 1205 and 1206 of the Emperor Seamounts (Ivarsson and Holm 2008; Ivarsson et al. 2008a, 2008b, 2012). In those publications the microorganisms were embedded and fossilized in hydrothermally formed carbonates. The mode of preservation of the filamentous structures described in this paper is quite different. They have not been entombed in hydrothermally formed minerals and, thus, it is difficult to correlate them with hydrothermal activity. However, their montmorillonite signature indicates that they must have been preserved and mineralized in an aquatic system of ambient or higher temperatures. Montmorillonite belongs to the suite of hydrothermally formed minerals observed in samples from ODP Leg 197 (Tarduno et al. 2002). Even though montmorillonite is a low-temperature mineral, the hydrothermal mineral succession is considered to be formed in close association with the volcanically active period or slightly after the hydrothermal activity subsided (Révillon et al. 2007). The basalts were subject to seawater alteration during 1–2 million years while the sediment pile built up and finally isolated the volcanic section from downward penetration of seawater (Révillon et al. 2007). The hydrothermal activity at the Emperor Seamounts ceased millions of years ago when the hotspot migrated towards it present-day position. Thus, it is most probable that the filamentous structures are contemporaneous with the hydrothermal activity and with the life span of the subsequently fossilized microorganisms described by Ivarsson et al. (2008a, 2008b, 2012).

(3) The fossilized filamentous structures are exceptionally well preserved and resemble known microbiological morphology. The long, curvilinear appearance with frequent

branching is common among most microorganisms (Ehrlich 2002). Septa, anastomoses and a mycelium-like network are consistent with fungal morphology (Deacon 1997; Smith and Read 1997; see Fig. 8 as a comparison to a live fungal mycelium). Their size further supports a fungal (rather than a prokaryotic) interpretation of these filamentous structures. Size, however, cannot be used as a distinct criterion to distinguish between prokaryotes and eukaryotes, since bacterial cells of millimetre size and filaments of centimetre length are known (Schulz and Jørgensen 2001). The morphology of the networks and their filamentous structures is indistinguishable from that of the fossilized fungal hyphae described by Ivarsson et al. (2012). Those fossilized fungi were observed in samples from site 1206 and were preserved in calcite. The fungi consisted of mycelium-like networks of fossilized hyphae with fungal characteristics such as septa, anastomosis and a central strand. Chitin was detected in the cell walls of some hyphae. The fossilized mycelia in this study further display characteristic fungal morphologies such as yeast-like growth and resting structures discussed in the following section: fungal structures.

(4) No chemical biomarkers indicative of life have been detected in the samples. EDS analyses revealed no traces of carbon in the filaments. If the filaments represent fossilized microorganisms, then the organic compounds must have been decomposed, probably by exposure to oxygenated conditions or bacteria. The high amount of organic remains in the fossilized microorganisms described by Ivarsson et al. (2008a, 2008b, 2012) was probably due to rapid mineral precipitation and entombment of the microorganisms.

(5) The filamentous structures occur without exception in colony-like assemblages that resemble fungal mycelia (Ehrlich 2002). Thus, this condition is fulfilled.

(6) It is difficult to conclude whether or not the filamentous structures show evidence of biomineralization. However, the montmorillonite is most likely the result of microbial clay authigenesis (Konhauser and Urrutia 1999), and not diagenetic in origin (see discussion in section below).

Evidently, the material meets the criteria for biogenicity, except criterion no. 4: no organic carbon was detected. The results are overall in favour of a biogenic rather than an abiotic interpretation. Thus, it is suggested that the filamentous structures are fossilized microorganisms. Because of characteristic fungal morphologies as well as the striking similarity to fossilized fungi described from samples from the same sites, the fossilized networks are proposed to represent fossilized fungal mycelia.

Fungal structures

The spherical and cluster-like structures associated with the fossilized hyphae described in this study could, within a fungal model, be interpreted as some sort of reproductive organ. However, they do not display any characteristic morphology of neither spores nor fruiting bodies (Deacon 1997; Smith and Read 1997). The size, morphology and occurrence of the smaller, spherical structures suggest unicellular yeast-like growth of some fungi. The smooth, indistinct transitions from filamentous hyphae to single yeast-like cells and the budding structures resemble fungi that are capable of switching from yeast to filamentous state or vice versa. Yeast-like growth among fungi can result in large irregular clusters with no apparent growth direction (Deacon 1997; Smith and Read 1997; Webster and Weber 2007).

The larger structures could be explained as fruiting bodies, but neither SRXTM nor optical microscopy showed any evidence that the structures contained spores, nor are they an assemblage of tightly packed fungal hyphae. An alternative interpretation would be that the subspherical clusters represent some type of resting structures like sclerotia. Sclerotia serve a survival function: they are formed as a response to environmental extremes and remain in dormant state until favourable conditions return (Webster and Weber 2007).

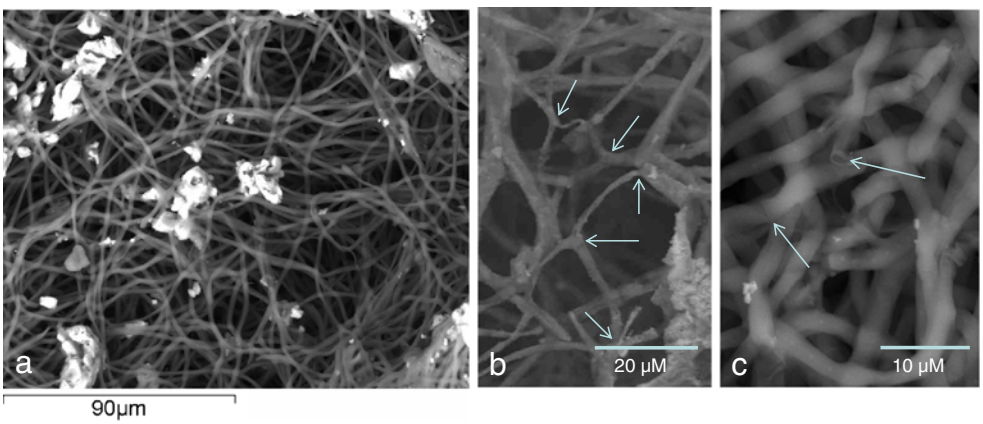

Fig. 8 ESEM images of a live mycelium from the subway station Kungsträdgården, Stockholm, Sweden. **a** Overview. **b** Anastomoses between branches (*arrows*). **c** Septa (*arrows*)

Sclerotia develop from an initial cluster of densely packed hyphae that undergoes structural changes, and differentiate into a solid, massive tissue. In highly developed sclerotia, walls are thickened and become melanised with an outer, well-defined rind-like layer. The morphology of the subspherical clusters described in this paper corresponds well to the morphological characteristics of sclerotia (Willetts and Bullock 1992; Willetts 1997), and it is probable that the environmental conditions of a subseafloor hydrothermal system would have forced the fungi to produce protective dormant structures for survival. An intriguing circumstance is also that sclerotia are found only among a small number of Asco- and Basidiomycota. Based on morphological features and the presence of chitin, Ivarsson et al. (2012) interpreted the fungi from the Emperor Seamounts as Ascomycota.

Preservation of subseafloor fungal colonies

The exceptional morphological and chemical preservation of the fossilized fungal hyphae described by Ivarsson et al. (2008a, 2008b) was explained as a direct result of instant mineral formation and entombment of the microorganisms (Ivarsson et al. 2009). The autolysis and decomposition of the microorganisms were inhibited by instant isolation by a mineral phase that protected the embedded fungal hyphae from contact with fluids, oxygen and decomposing microorganisms. Absence of later metamorphism also is important for preservation of the embedded microorganisms. The preservation of the fossilized fungal hyphae described in this paper is exceptional as well, despite the lack of an embedding mineral, and they display several similarities to the fossilized hyphae described by Ivarsson et al. (2008a, 2008b, 2012), except in the lack of organic remains. This indicates that the preservation of organic remains is dependent on complete entombment by a mineral phase. The morphology, on the other hand, is almost as well preserved as in the fossilized microorganisms entombed in calcite. Evidently, the replacement with montmorillonite has preserved the main morphological features and has also given the fossilized hyphae sufficient stability to avoid collapse. The exceptional preservation of the morphology of the whole mycelium suggests that the fossilization and replacement with montmorillonite must have begun while the organisms were still alive. If the replacement had occurred after death, the mycelium would have collapsed and become dehydrated. At death fungal hyphae become dehydrated, resulting in flat hyphae, not circular as in the present study (Deacon 1997; Smith and Read 1997).

Montmorillonite was probably precipitated or localized on the surfaces of the hyphae while the fungi were alive. Interaction between fungi and clay is a well-known phenomenon (Gadd 2007). Fungal production of extracellular mucilaginous substances stimulates accumulation of inorganic compounds and subsequent precipitation of clay-like phases or oxides. If a considerable amount of inorganic material is deposited onto the fungal hyphae, then decomposition can be inhibited, and fossilization and preservation stimulated. Whole colonies can, in fact, be "mummified" (Gorbushina et al. 2002). Fungi in subaerial rock environments—like hot and cold deserts with varying extremes in microclimatic conditions including irradiation, salinity, pH, humidity and temperature—protect themselves by producing extracellular polymeric substances (EPS) and/or mucilaginous polysaccharides that contain clay particles (Gorbushina 2003; Volkmann et al. 2003; Gadd 2007). Under extreme conditions, whole colonies can be embedded in such clay-containing mucilaginous precipitates.

Although extreme in nature, hydrothermal systems are not directly comparable to subaerial desert environments. Hydrothermal systems are dynamic environments, where shifts in temperature, pH, toxicity and nutrient supply can occur rapidly. Such changes might force adaptability upon resident microorganisms with regard to survival strategies and metabolic activity. It is most likely that the fungi described in this study have been forced to protect themselves from environmental stress by producing EPS/mucilaginous polysaccharides that stimulated precipitation and/or deposition of inorganic clay-like phases that subsequently crystallized to montmorillonite. If they were contemporaneous with the fossilized fungi described by Ivarsson et al. (2012), they would have been subject to pulses of hotter fluids with temperatures over 100 °C for some periods of time (Ivarsson et al. 2009). Evidence of thick cell walls revealed by the present study as well as by Ivarsson et al. (2012) indicates a protective strategy. Thick hyphal cell walls are often developed among fungi that are exposed to environmental stress, such as high temperatures. This is known, for instance, from microcolonial fungi, a unique type of stress-tolerant fungi found in desert environments characterized by extreme conditions (Staley et al. 1982; Gorbushina 2007).

The results of this study suggest that the search for fossilized microorganisms in subseafloor environments should not only be restricted to filled pore spaces but also include open fractures. By detailed studies and careful interpretation, it should be possible to establish biogenicity of microfossils observed in such micro-niches.

Conclusions

Fossilized networks of filamentous microorganisms observed in vesicles of subseafloor basalts from the Emperor Seamounts, Pacific Ocean, have been examined with optical microscopy, ESEM/EDS, XRD as well as SRXTM, and interpreted as fossilized fungal mycelia. These mycelia consist mainly of interconnected hyphae, but yeast-like growth states occur as well. They are almost identical in appearance to fossilized fungi described in related samples from the Emperor Seamounts (Ivarsson et al. 2012), except that the

latter have been entombed in a secondary carbonate phase. The fossilized fungi described here occur in open or partially filled vesicles and are mineralized with montmorillonite. The precipitation or deposition of montmorillonite likely begun while the fungi were alive as a result of a protective strategy by which the fungi produced mucilaginous polysaccharides or EPS that favoured precipitation of clay minerals or attracted clay particles. This resulted in complete fossilization by montmorillonite. Large, spherical structures associated with the hyphae are similar to resting structures, sclerotia, found among other fungi that live in extreme environments. Subseafloor settings are highly variable environments, which force survival strategies upon microbial colonies. This study introduces open pore spaces in subseafloor basalts as a new micro-niche where fossilized microorganisms can be found.

Acknowledgments We wish to thank Marianne Ahlbom at the Department of Geological Sciences, Stockholm University, for ESEM analysis. The SRXTM investigations were conducted at the X02DA (TOMCAT) beamline of the Swiss Light Source, Paul Scherrer Institute. This work was funded by the Swedish National Space Board. Constructive comments by J. Peckmann and two anonymous reviewers proved useful in improving the manuscript.

References

Al-Hanbali HS, Sowerby SJ, Holm NG (2001) Biogenicity of silicified microbes from a hydrothermal system: relevance to the search for life on Earth and other planets. Earth Planet Sci Lett 191:213–218

Buick R (1991) Microfossil recognition in Archean rocks: an appraisal of spheroids and filaments from a 3500 m.y. old chert-barite unit at North Pole, Western Australia. Palaios 5:441–459

Cavalazzi B, Westall F, Cady SL, Barbieri R, Foucher F (2011) Potential fossil endoliths in vesicular pillow basalt, Coral Patch Seamount, Eastern North Atlantic Ocean. Astrobiology 11:619–632

Deacon JW (1997) Modern mycology. Wiley Blackwell, Oxford

Donoghue PCJ, Bengtson S, Dong X-P, Gostling NJ, Huldtgren T, Cunningham JA, Yin C, Yue Z, Peng F, Stampanoni M (2006) Synchrotron X-ray tomographic microscopy of fossil embryos. Nature 442:680–683

Ehrlich HL (2002) Geomicrobiology. Marcel Dekker, New York

Eickmann B, Bach W, Kiel S, Reitner J, Peckmann J (2009) Evidence for cryptoendolithic life in Devonian pillow basalts of Variscan orogens, Germany. Palaeogeogr Palaeoclim Palaeoecol 283:120–125

Furnes H, McLoughlin N, Muehlenbachs K, Banerjee N, Staudigel H, Dilek Y, de Wit M, Van Kranendonk M, Schiffman P (2008) Oceanic pillow lavas and hyaloclastites as habitats for microbial life through time – a review. In: Dilek Y, Furnes H, Muehlenbachs K (eds) Links between geological processes, microbial activities and evolution of life. Springer, Berlin, pp 1–68

Gadd GM (2007) Geomycology: biogeochemical transformations of rocks, minerals, metals and radionuclides by fungi, bioweathering and bioremediation. Mycol Res 111:3–49

Gibson EK, McKay DS, Thomas-Keptra KL, Wentworth SJ, Westall F, Steele A, Romanek CS, Bell MS, Toporski J (2001) Life on Mars: evaluation of the evidence within Martian meteorites ALH84001, Nakhla, and Shergotty. Precamb Res 106:15–34

Gorbushina A (2003) Microcolonial fungi: survival potential of terrestrial vegetative structures. Astrobiology 3:543–554

Gorbushina A (2007) Life on the rocks. Environ Microbiol 9:1613–1631

Gorbushina AA, Krumbein WE, Volkmann M (2002) Rock surfaces as life indicators: new ways to demonstrate life and traces of former life. Astrobiology 2:203–213

Ivarsson M (2006) Advantages of doubly polished thin sections for the study of microfossils in volcanic rock. Geochem Trans 7:5

Ivarsson M (2012) Subseafloor basalts as fungal habitats. Biogeosciences 9:3625–3635

Ivarsson M, Holm NG (2008) Microbial colonization of various habitable niches during alteration of oceanic crust. In: Dilek Y, Furnes H, Muehlenbachs K (eds) Links between geological processes, microbial activities and evolution of life. Springer, Berlin, pp 69–111

Ivarsson M, Lindblom S, Broman C, Holm NG (2008a) Fossilized microorganisms associated with zeolite-carbonate interfaces in sub-seafloor hydrothermal environments. Geobiology 6:155–170

Ivarsson M, Lausmaa J, Lindblom S, Broman C, Holm NG (2008b) Fossilized microorganisms from the Emperor Seamounts: implications for the search for a subsurface fossil record on Earth and Mars. Astrobiology 8:1139–1157

Ivarsson M, Broman C, Lindblom S, Holm NG (2009) Fluid inclusions as a tool to constrain the preservation conditions of sub-seafloor cryptoendoliths. Planet Space Sci 57:477–490

Ivarsson M, Bengtson S, Belivanova V, Stampanoni M, Marone F, Tehler A (2012) Fossilized fungi in subseafloor Eocene basalts. Geology 40:163–166

Konhauser KO, Urrutia MM (1999) Bacterial clay authigenesis: a common biogeochemical process. Chem Geol 161:399–413

Lysnes K, Thorseth IH, Steinsbau BO, Øvreås L, Torsvik T, Pedersen RB (2004) Microbial community diversity in seafloor basalt from the Arctic spreading ridges. FEMS Microbiol Ecol 50:213–230

Marone F, Stampanoni M (2012) Regridding reconstruction algorithm for real-time tomographic imaging. J Synchrotron Rad 19:1029–1037

McLoughlin N, Furnes H, Banerjee NR, Muehlenbachs K, Staudigel H (2009) Ichnotaxonomy of microbial trace fossils in volcanic glass. J Geol Soc 166:159–169

Peckmann J, Bach W, Behrens K, Reitner J (2008) Putative cryptoendolithic life in Devonian pillow basalt, Rheinisches Schiefergebirge, Germany. Geobiology 6:125–135

Révillon S, Teagle DAH, Boulvais P, Shafer J, Neal CR (2007) Geochemical fluxes related to alteration of a subaerially exposed seamount: Nintoku seamount, ODP Leg 197, Site 1205. Geochem Geophys Geosyst 8:1–26

Santelli CM, Orcutt BN, Banning E, Bach W, Moyer CL, Sogin ML, Staudigel H, Edwards KJ (2008) Abundance and diversity of microbial life in ocean crust. Nature 453:653–657

Schopf JW, Walter MR (1983) Archean microfossils: new evidence of ancient microbes. In: Schopf JW (ed) Earth's earliest biosphere, its origin and evolution. Princeton University Press, Princeton, pp 214–239

Schulz HN, Jørgensen BB (2001) Big bacteria. Annu Rev Microbiol 55:105–137

Schumann G, Manz W, Reitner J, Lustrino M (2004) Ancient fungal life in North Pacific Eocene oceanic crust. Geomicrobiol J 21:241–246

Smith SE, Read OJ (1997) Mycorrhiza symbiosis. Academic Press, London

Staley JT, Palmer F, Adams JB (1982) Microcolonial fungi: common inhabitants on desert rocks? Science 215:1093–1095

Stampanoni M, Groso A, Isenegger A, Mikuljan G, Chen Q, Bertrand A, Henein S, Betemps R, Frommherz U, Böhler P, Meister D, Lange M, Abela R (2006) Trends in synchrotron-based tomographic imaging: the SLS experience. Proc SPIE 6318, Developments in X-Ray Tomography V, 63180 M. doi:10.1117/12.679497

Staudigel H, Furnes H, McLoughlin N, Banerjee NR, Connell LB, Templeton A (2008) 3.5 billion years of glass bioalteration: volcanic rocks as a basis for microbial life? Earth Sci Rev 89:156–176

Tarduno JA, Duncan RA, Scholl DW (2002) Leg 197 summary. Proc ODP, Init Rep 197:1–92

Thorseth IH, Torsvik T, Torsvik V, Daae FL, Pedersen RB, Keldysh-98 Scientific Party (2001) Diversity of life in ocean floor basalt. Earth Planet Sci Lett 194:31–37

Thorseth IH, Pedersen RB, Christie DM (2003) Microbial alteration of 0-30-Ma seafloor basaltic glasses from the Australian Antarctic Discordance. Earth Planet Sci Lett 215:237–247

Volkmann M, Whitehead K, Rutters H, Rullkötter J, Gorbushina AA (2003) Mycosporine-glutamicol-glucoside: a natural UV-absorbing secondary metabolite of rock-inhabiting microcolonial fungi. Rapid Commun Mass Spectrom 17:897–902

Webster J, Weber RWS (2007) Introduction to fungi, 3rd edn. Cambridge University Press, Cambridge

Willetts HJ (1997) Morphology, development and evolution of stromata/sclerotia and macroconidia of the Sclerotiniaceae. Mycol Res 101:939–952

Willetts HJ, Bullock S (1992) Developmental biology of sclerotia. Mycol Res 96:801–816